Matrix Isolation Infrared and ab Initio Study of Formic Acid−Acetylene Interaction: Example of H···π and C−H···O Interaction

Lisa George, Elsa Sanchez-García, and Wolfram Sander*

Lehrstuhl für Organische Chemie II der Ruhr-Universität Bochum, D-44780 Bochum, Germany

Received: January 21, 2003; In Final Form: May 30, 2003

The hydrogen-bond interaction between formic acid and acetylene was studied by matrix isolation infrared spectroscopy coupled with ab initio computations. The 1:1 adduct of formic acid and acetylene was isolated in argon matrix, and the adduct formation was evidenced by the perturbation in the formic acid and acetylene vibrational modes. The structures, binding energies, and vibrational frequencies were calculated at the MP2 and B3LYP levels of theory using the 6-311++G(d,p) and aug-cc-pVTZ basis sets. Three minima corresponding to formic acid−acetylene complexes were identified at the highest level of theory (MP2/aug-cc-pVTZ). All of the three structures are cyclic with two hydrogen-bond interactions. In the global minimum complex A, the hydrogen atom in the carboxyl group of formic acid interacts with the π-system of acetylene (O−H···π). The second interaction is between one of the hydrogen atoms of acetylene and the carbonyl oxygen atom of formic acid. In the second complex B, the hydrogen bonding is a ≡C−H···O interaction involving a hydrogen atom of acetylene and the carbonyl oxygen atom of formic acid. In the second interaction, the formyl hydrogen atom of formic acid interacts with the π-system of acetylene. In the third complex C, the main interaction involves one of the hydrogen atoms of acetylene and the hydroxyl oxygen atom of formic acid. In this complex, there is also a secondary interaction between the formyl hydrogen atom of formic acid and the π-system of acetylene. This latter interaction is not reproduced using DFT calculations. The stabilization energy for the global minimum A is −4.9 kcal/mol, for the second complex B it is −2.9 kcal/mol, and that for the third complex C is −2.0 kcal/mol at the MP2/aug-cc-pVTZ level of calculation, corrected for the basis set superposition error (BSSE) using the Boys−Bernardi counterpoise scheme. The two most stable complexes A and B were identified in argon matrixes using FTIR spectroscopy. The calculated IR spectra of these complexes are in good agreement with the experimental spectra. Experiments with deuterated acetylene were performed to confirm the band assignments. The calculated frequency shift for the O−H stretching vibration of formic acid (−139 cm^{-1} at MP2/aug-cc-pVTZ) is in excellent agreement with the experimental shift (−137 cm^{-1}) for the O−H···π complex A. This large shift in the O−H stretching vibration is a strong evidence for the O−H···π interaction, which is consistent with the predicted large binding energy.

Introduction

The hydrogen bond is the most significant intermolecular interaction responsible for a large number of chemical and biological processes.[1,2] Conventional strong hydrogen bonds such as OH···O, NH···O, and OH···N have been extensively studied.[3−6] The weak or nonconventional hydrogen bonding, such as CH···O and H···π interactions, are of considerable interest in recent years because of the significant role they play in determining the shapes and stabilities of proteins and crystal structures.[7−9] There are many experimental and theoretical studies of C−H···X complexes, where X can be various proton acceptors such as O, N, halogens, and π systems.[10−12] The matrix isolation technique has been extensively used to study the hydrogen-bonded complexes of alkynes and alkenes with several oxygen and nitrogen bases by Ault and co-workers.[13−15] Hydrogen-bonded complexes of X−H···π, in which the hydride acts as proton donor toward the π system of benzene-, acetylene-, or ethylene-type systems were also investigated by many authors.[16,17] The present study focuses on the matrix isolation infrared and ab initio study of hydrogen bonds formed between acetylene and formic acid. In this system O−H···π and ≡C−H···O interactions are the two dominating hydrogen bonds. Our ab initio computation indicates that the O−H···π interaction is energetically more favorable than the ≡C−H···O interaction. The weak C−H···π interaction also plays an important role for the stabilization. The geometries, energies, and vibrational frequencies of the 1:1 complexes of the formic acid−acetylene system are described here.

Experimental Section

Matrix isolation experiments were performed by standard techniques using an APD CSW-202 Displex closed-cycle helium refrigerator. Spectroscopic-grade formic acid (Acros Organics) and acetylene/deuterated acetylene gas were premixed with argon gas in a mixing chamber made of glass, using the standard manometric method. Formic acid was degassed several times by the freeze-pump-thaw method before mixing with argon. About 1−4 mbar of acetylene/deuterated acetylene gas was mixed with 0.5−2 mbar of formic acid and diluted with 800 mbar of argon in a 2-L glass bulb. Deposition was done on a CsI substrate held at 15 K. The matrix was annealed at 25 and 30 K by keeping at that temperature for 20 min and cooled to 14 K before recording the annealed spectra. Spectra were

* To whom correspondence should be addressed. E-mail: wolfram.sander@rub.de.

10.1021/jp034158s CCC: $25.00
Published on Web 08/13/2003

recorded with a Bruker (Equinox 55 and IFS/66V) FTIR spectrometer at 0.5 cm^{-1} resolution in the range of 400−4000 cm^{-1}, and 128 scans were coadded.

Computational Methods

Ab initio computations were performed using the Gaussian 98 program suite.[18] The equilibrium geometries and vibrational frequencies were calculated with the Møller−Plesset perturbation theory of second order (MP2)[19] and density functional theory (DFT) method with the B3LYP hybrid functional.[20,21] At both the MP2 and DFT level of calculations, a triple-ζ basis set added with diffuse functions and polarization functions (6-311++G(d,p))[22,23] and also Dunning's correlation-consistent triple-ζ basis set[24] augmented with diffuse functions were used.

To evaluate the effect of the basis set size, both the Pople's and Dunning's basis sets were used at both the MP2 and DFT levels. The stabilization energies were calculated at the MP2 level by subtracting the energies of the monomers from those of the complexes, and those energies were corrected for the basis set superposition errors (BSSE) using the counterpoise (CP) scheme of Boys and Bernardi.[25]

To localize the minima for the formic acid−acetylene system, we have used the multiple minima hypersurface (MMH) approach,[26,27] which combines the quantum chemical procedures for calculating the cluster energies in local minima geometry of supermolecules and the statistical thermodynamics approach for the evaluation of macroscopic properties. It is not our purpose to outline here the theoretical grounds of this approach because they have been already described previously.

In this way, several arbitrary arrangements of acetylene−formic acid have been taken as starting point, and a traditional gradient minimization procedure with respect to the cluster Hamiltonians was used. Around 1000 randomly arranged formic acid−acetylene clusters were generated as starting point, and the results were processed with two programs especially written for this purpose. For building starting clusters, a single molecule of acetylene was placed in the center of coordinates and taken as input data. An additional formic acid molecule was placed on a new randomly positioned center of coordinates (with respect to the one of the initial molecule) and was rotated, also randomly, around the three coordinate axis.

Thus, the procedure involves a large number of molecular arrangements during the gradient-driven path to explore the multiple minima hypersurface (MMH) of such systems. The path followed lead to local minima of potential energy of the molecular cluster.

To calculate the energies of all these previous molecular arrangements, we used an approximate quantum mechanical Hamiltonian. After that, we used the programs already mentioned above[28] to process the results of the semiempirical calculations and perform the similarity analysis. It becomes necessary to consider that there are two types of degeneracy in this kind of hypersurface minima. The first consists of clusters that are identical, that is, they have both the same energy and molecular geometry, and we call it as similarity degeneracy (SD). The second consists of clusters with different molecular geometry but the same energy, and we call it as valid degeneracy (VD). The program contains a subroutine called Tanimoto to analyze the similarity among molecular arrangements to discard SD. Then, after calculating around 1000 supermolecular geometries, we find the relevant semiempirical local formic acid−acetylene minima. It is important to point out that these semiempirical results provide a preliminary overview of the formic acid−acetylene interactions. For this reason, the minima have been refined using DFT and MP2 methods.

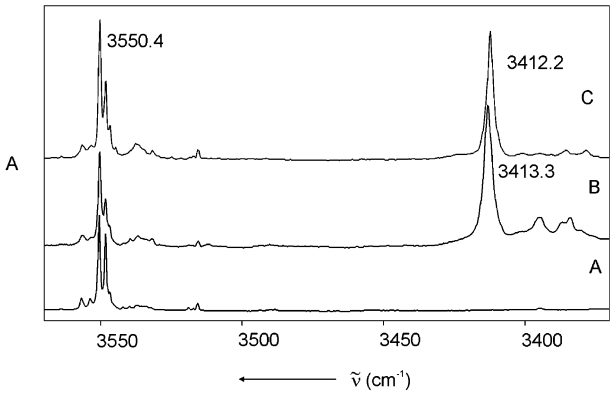

Figure 1. Matrix isolation infrared spectra in the O−H stretching region of formic acid: (A) HCOOH−Ar (1:600); (B) HCOOH−C_2H_2−Ar (1:2:600); (C) HCOOH−C_2D_2−Ar (1:2:600).

Results and Discussion

Experimental Results. The infrared spectra of formic acid isolated in rare gas matrixes have been reported earlier.[29−34] Vibrational modes corresponding to O−H, C═O, and C−O stretch are of main consideration for the molecular interaction studies of formic acid complexes. To identify the formic acid−acetylene complex spectra, infrared spectra of pure formic acid and acetylene were recorded independently by depositing matrixes with argon-to-sample ratios ranging from 1000:1 to 300:1. The blank spectra of formic acid and acetylene in solid argon agree well with spectra reported in the literature.[29,35,36] Figure 1 displays the OH stretching region of formic acid in three different sets of experiments. The spectrum marked "A" corresponds to a 1:600 molar ratio of formic acid and argon deposited at 15 K and subsequently annealed at 30 K. The peak observed at 3550.4 cm^{-1} is assigned to the OH stretching vibration of formic acid. The splitting of this band is caused by site effects in the argon matrix.[37] On codeposition of formic acid, acetylene, and argon in a 1:2:600 molar ratio, a new distinct feature appears at 3413.3 cm^{-1} (Figure 1B), red-shifted by 137 cm^{-1} from the unperturbed OH mode of formic acid. Increasing the acetylene concentration or annealing the matrix for several minutes at 25−30 K to allow diffusion of the trapped species results in an increase in the intensity of this band. This clearly shows that this absorption is due to a formic acid−acetylene complex. The peak at 3413.3 cm^{-1} appears even at low concentrations of formic acid and acetylene, and hence, it is attributed to a 1:1 complex of formic acid and acetylene. The spectrum C was obtained by codeposition of formic acid and deuterated acetylene.

Figure 2 displays the C═O stretching region of formic acid in three different experiments. The spectrum marked "A" corresponds to a 1:600 molar ratio of formic acid and argon deposited at 15 K and annealed at 30 K following the deposition. The peak at 1767.1 cm^{-1} with a shoulder at 1764.8 cm^{-1} is assigned to the C═O stretching vibration of formic acid. The weak absorptions at 1747 and 1728 cm^{-1} are assigned to the acyclic and cyclic forms of the formic acid dimer.[34] Even at high dilution of formic acid, these characteristic dimer absorptions were observed. On codeposition of formic acid, acetylene, and argon in a 1:2:600 molar ratio, a new band appeared at 1756.6 cm^{-1} (Figure 2B). On increase of the acetylene concentration and also after the matrix was annealed at 30 K, this band gained in intensity, revealing that this spectral feature

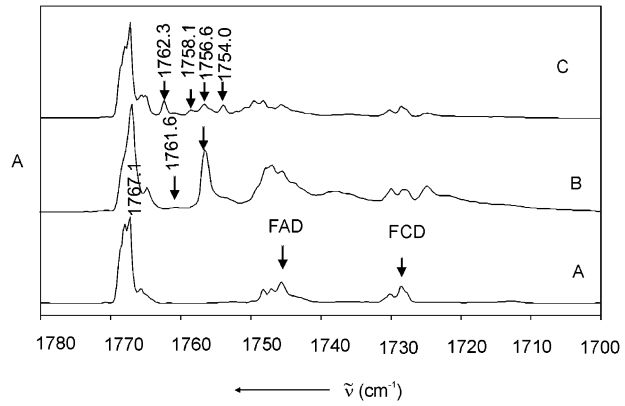

Figure 2. Matrix isolation infrared spectra in the C═O stretching region of formic acid: (A) HCOOH−Ar (1:600); (B) HCOOH−C_2H_2−Ar (1:2:600); (C) HCOOH−C_2D_2−Ar (1:2:600). FAD indicates formic acid acyclic dimer; FCD indicates formic acid cyclic dimer.

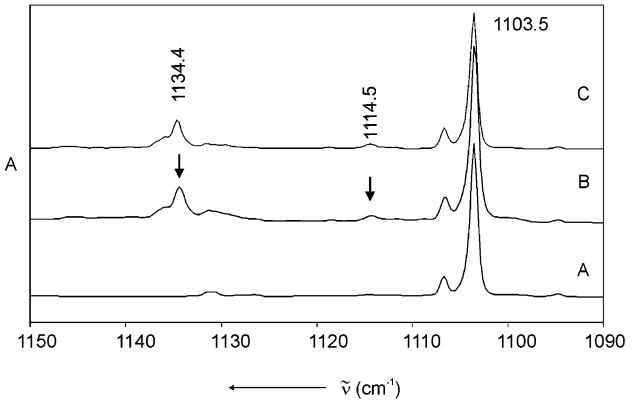

Figure 3. Matrix isolation infrared spectra in the C−O stretching region of formic acid: (A) HCOOH−Ar (1:600); (B) HCOOH−C_2H_2−Ar (1:2:600); (C) HCOOH−C_2D_2−Ar (1:2:600).

is due to formic acid−acetylene complex. Even at low concentrations of formic acid and acetylene, the peak at 1756.6 cm^{-1} appears, and hence, it is attributed to a perturbed C═O stretching mode of the 1:1 complex of formic acid and acetylene. In the C═O stretching region of formic acid in the presence of acetylene, another weak feature is observed at 1761.6 cm^{-1}, red-shifted by 6 cm^{-1} from the free formic acid. In Figure 2C, the spectra obtained by codeposition of formic acid, deuterated acetylene, and argon in a 1:2:600 molar ratio are displayed. Because the deuterated acetylene contains also C_2DH and C_2H_2, additional peaks of the corresponding isotopomers are found at 1758.1, 1756.6, 1754.0, and 1762.3 cm^{-1}.

In the C−O stretching region of formic acid, a new distinct band is observed at 1134.4 cm^{-1} (Figure 3B), which is 31 cm^{-1} blue-shifted from the unperturbed C−O stretching vibration at 1103.5 cm^{-1}. An additional weak absorption is observed at 1114.5 cm^{-1}. Both new bands seem to be a perturbed mode of the C−O stretching vibration. The corresponding spectra obtained with deuterated acetylene are shown in Figure 3C. Acetylene, in contrast to formic acid, does not exhibit any absorption in this region.

In the presence of formic acid, the vibrational modes of acetylene are also perturbed. The C−H stretching mode (ν_3) of acetylene is observed at 3288.8 cm^{-1} and the ($\nu_2 + \nu_4 + \nu_5$) mode is found at 3302.9 cm^{-1}, as reported in the literature.[35] The other weak bands at around 3285, 3269, and 3265 cm^{-1} are due to acetylene dimers (Figure 4A).[35,36,38] The weak band at 3240 cm^{-1} has been assigned to a complex between acetylene and water by Engdahl and Nelander.[39] When acetylene and

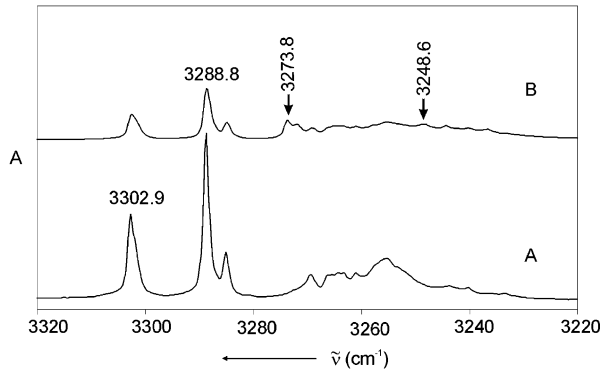

Figure 4. Matrix isolation infrared spectra in the C−H stretching region of acetylene: (A) C_2H_2−Ar (1:300); (B) HCOOH−C_2H_2−Ar (1:2:600).

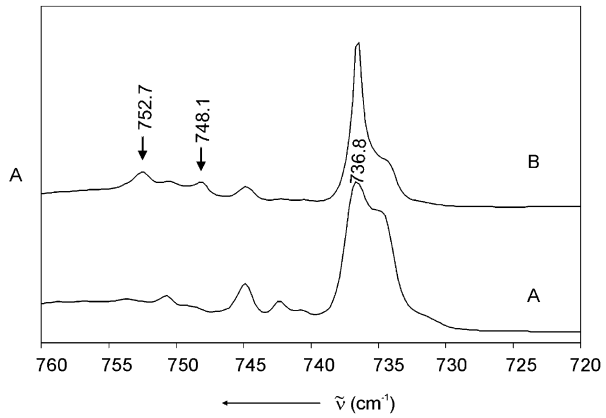

Figure 5. Matrix isolation infrared spectra in the CCH bending region of acetylene: (A) C_2H_2−Ar (1:300); (B) HCOOH−C_2H_2−Ar (1:2:600).

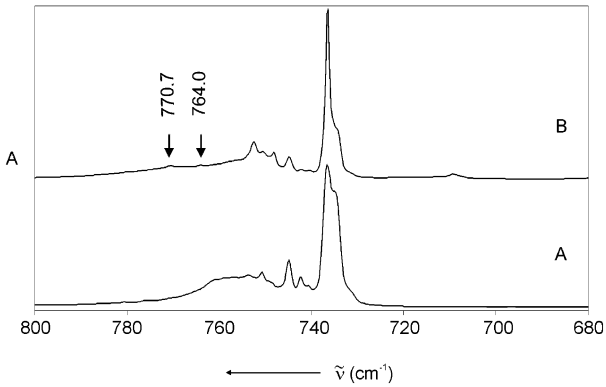

Figure 6. Matrix isolation infrared spectra in the CCH bending region of acetylene (ordinate expanded): (A) C_2H_2−Ar (1:300); (B) HCOOH−C_2H_2−Ar (1:2:600).

formic acid are codeposited, a few new bands are observed: a doublet at 3273.8 and 3272.2 cm^{-1} and another weak band at 3248.6 cm^{-1} (Figure 4B). The intensity of these new absorptions depends on the formic acid concentration, indicating that these are due to formic acid−acetylene complexes. In the CCH bending region of acetylene, the ν_5 band occurs as a doubly degenerate mode at 736.8 cm^{-1}, and two satellites were also present at 744.7 and 750.8 cm^{-1} as reported earlier (Figure 5A).[36] On codeposition of formic acid with acetylene, two new bands at 748.1 and 752.7 cm^{-1} appear (Figure 5B). Two additional very weak bands appear at 764.0 and 770.7 cm^{-1} (Figure 6B). From the dependence of these new absorptions on the concentrations of both components, it can be concluded that a 1:1 complex of formic acid and acetylene is formed.

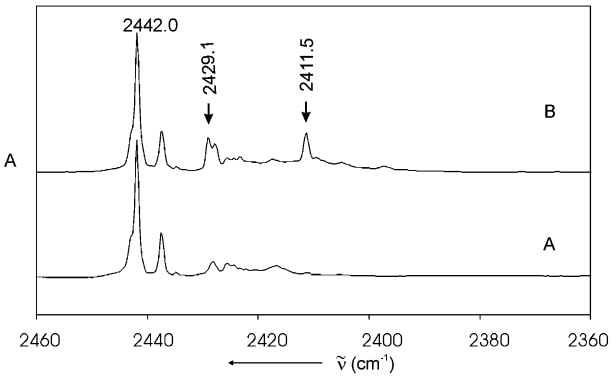

Figure 7. Matrix isolation infrared spectra in the C−D stretching region of deuterated acetylene: (A) C_2D_2−Ar (1:300); (B) HCOOH−C_2D_2−Ar (1:2:600).

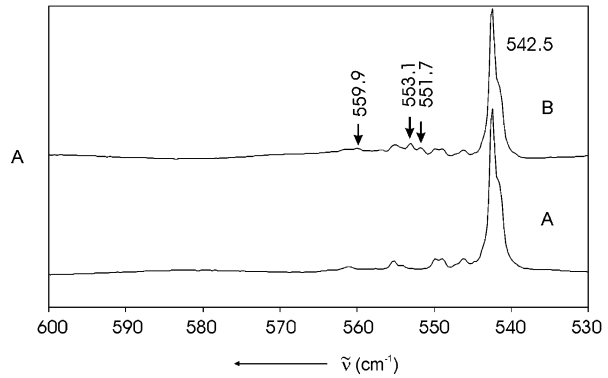

Figure 8. Matrix isolation infrared spectra in the CCD bending region of deuterated acetylene: (A) C_2D_2−Ar (1:300); (B) HCOOH −C_2D_2−Ar (1:2:600).

With deuterated acetylene, the CD stretching mode (ν_3) of C_2D_2 is observed at 2442.0 cm^{-1}, with additional complex patterns observed at 2429.1, 2428.1 (doublet), and 2411.5 cm^{-1} (Figure 7B). In the CCD bending region, the ν_5 band occurs as a doubly degenerate mode at 542.5 cm^{-1} with two satellites at 548.8 and 555.1 cm^{-1}. On codeposition of formic acid with deuterated acetylene, two new bands appear at 551.7 and 553.1 cm^{-1} (Figure 8B). An additional very weak band is found at 559.9 cm^{-1} (Figure 8B). Again, the dependence of peak intensities on the ratio of the two components suggests the formation of a 1:1 complex.

Computational Results: Structures and Binding Energies of the Complexes. The structures obtained with the MP2 and DFT methods and both the aug-cc-pVTZ and 6-311++G(d,p) basis sets are shown in Figure 9. At the MP2/aug-cc-pVTZ level of theory, three stable complexes with cyclic structures have been identified (structures A, B, and C). All three complexes have C_s symmetries. At the MP2/6-311++G(d,p) level, two additional complexes with monodentate structures (B1 and C1) are also obtained. Vibrational frequency calculations ensured that all five complexes correspond to minima on the potential energy surface. In the global minimum structure A (Figure 9A), the acidic hydrogen atom of formic acid approaches nearly perpendicular to the π-electron density of the triple bond of acetylene. The O−H···C_1 distance is 2.403 Å and the O−H···C_2 distance is 2.235 Å at the MP2/aug-cc-pVTZ level. MP2/6-311++G(d,p) calculations predict an O−H···C_1 distance of 2.466 Å and an O−H···C_2 distance of 2.329 Å. The distance from the OH hydrogen atom to the center of the carbon−carbon triple bond is 2.216 Å with MP2/aug-cc-pVTZ and 2.304 Å with MP2/6-311++G(d,p) theory. These distances are consistent with typical hydrogen-bond interactions. Thus, the hydrogen-bond distances in π-complexes of acetylene with HF and H_2O are 2.186 and 2.443 Å, respectively, at the MP2/6-311++G(d,p) level.[40] In addition, there is a weak C−H···O interaction, showing a hydrogen-bonding distance of 2.608 and 2.733 Å, respectively, at the MP2/aug-cc-pVTZ and MP2/6-311++G(d,p) level of theory. This second hydrogen bond results in a cyclic structure and an additional stabilization of the complex.

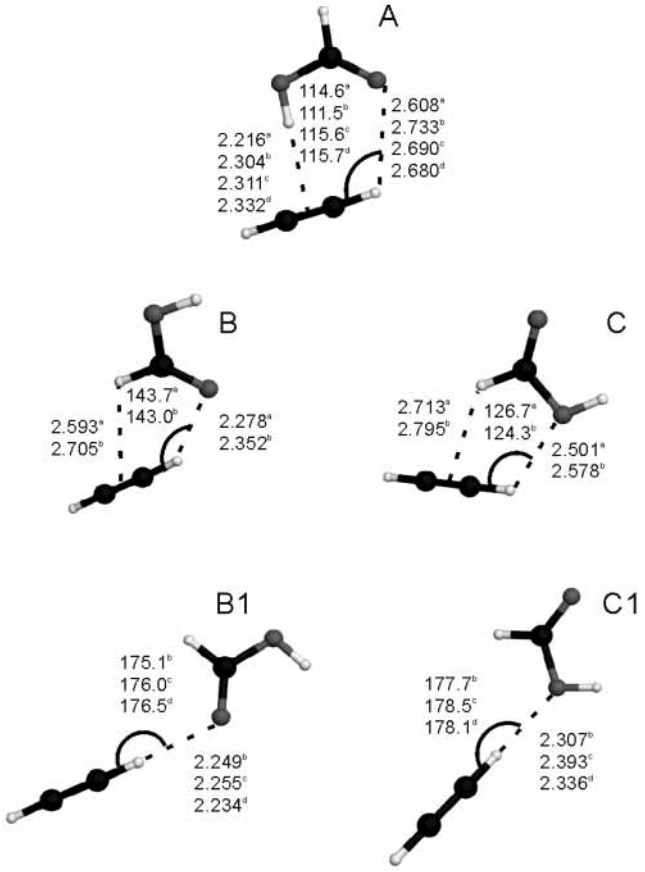

Figure 9. The calculated structures with hydrogen-bond lengths and hydrogen-bond angles of formic acid−acetylene complexes: (A) O−H···π bidentate; (B) ≡C−H···O=C bidentate; (C) ≡C−H···O−H bidentate; (B1) ≡C−H···O=C monodentate; (C1) ≡C−H···O−H monodentate; (a) MP2/aug-cc-pVTZ; (b) MP2/6-311++G(d,p); (c) B3LYP/aug-cc-pVTZ; (d) B3LYP/6-311++G(d,p).

The global minimum structure obtained with the B3LYP method closely resembles the MP2 structure. The distance from the OH hydrogen atom to the center of the carbon−carbon triple bond is 2.311 and 2.332 Å at the B3LYP/aug-cc-pVTZ and B3LYP/6-311++G(d,p) level, respectively. Because O−H···π is the main interaction in the formic acid−acetylene complex A, we address structure A as O−H···π complex for the further discussion.

The computed binding energies (ΔE), the BSSE-corrected ΔE, and the ZPE-corrected binding energies of all of the complexes computed with MP2/aug-cc-pVTZ and MP2/6-311++G(d,p) are given in Table 1. The binding energy of the O−H···π complex A, using MP2/aug-cc-pVTZ, is −5.4 kcal/mol and after BSSE correction is −4.9 kcal/mol. The binding energy reported for the water dimer at the same level of theory (MP2/aug-cc-pVTZ) is −4.6 kcal/mol after BSSE correction.[41] Compared to the water dimer, the stabilization of complex A is higher by −0.3 kcal/mol, an evidence for the strong interaction between formic acid and acetylene. After the ZPE correction (0.9 kcal/mol), the binding energy drops to −4.0 kcal/mol. The uncorrected binding energy obtained using MP2/6-311++G-

TABLE 1: Calculated MP2 Binding Energies, Uncorrected, BSSE-Corrected, and ZPE-corrected (in kcal/mol), of the Formic Acid−Acetylene Complexes

	MP2/aug-cc-pVTZ			MP2/6-311G++(d,p)		
complex	ΔE	$\Delta E_{(BSSE)}$	$\Delta E_{(ZPE)}$	ΔE	$\Delta E_{(BSSE)}$	$\Delta E_{(ZPE)}$
O−H···π bidentate (A)	−5.4	−4.9	−4.5	−4.7	−3.4	−3.9
C−H···O═C bidentate (B)	−3.3	−2.9	−2.6	−2.9	−2.2	−2.2
C−H···O═C monodentate (B1)				−2.9	−2.1	−1.9
C−H···O−H bidentate (C)	−2.3	−2.0	−1.8	−2.2	−1.5	−1.7
C−H···O−H monodentate (C1)				−2.2	−1.3	−1.2

TABLE 2: Calculated DFT/B3LYP Binding Energies, Uncorrected and ZPE-Corrected (in kcal/mol), of the Formic Acid−Acetylene Complexes

	B3LYP/aug-cc-pVTZ		B3LYP/6-311++G(d,p)	
complex	ΔE	$\Delta E_{(ZPE)}$	ΔE	$\Delta E_{(ZPE)}$
O−H···π bidentate (A)	−3.5	−2.7	−3.5	−2.7
C−H···O═C monodentate (B1)	−2.2	−1.6	−2.4	−1.7
C−H···O−H monodentate (C1)	−1.0	−0.5	−1.4	−0.7

(d,p) is −4.7 kcal/mol, which is 0.7 kcal/mol less compared to MP2/aug-cc-pVTZ. After the BSSE and ZPE correction, the binding energy drops to −2.6 kcal/mol, which is 1.4 kcal/mol less than the energy calculated using Dunning's correlation-consistent basis set aug-cc-pVTZ. This result shows that the MP2 interaction energy for complex A greatly depends on the basis set used in the calculation.

Table 2 lists the binding energies obtained with B3LYP/aug-cc-pVTZ and B3LYP/6-311++G(d,p) calculations. The DFT-calculated binding energies are more dependent on the basis set used and with approximately −3.5 kcal/mol (−2.7 kcal/mol including ZPE) are considerably smaller than the MP2 energies (Table 1).

As seen from Figure 9B, complex B also exhibits a cyclic structure: a ≡C−H···O interaction in which acetylene is the proton donor and the carbonyl oxygen of formic acid is the proton acceptor and a secondary interaction in which the formyl hydrogen atom of formic acid interacts with the π-system of acetylene. The hydrogen-bond distance is 2.278 Å using MP2/aug-cc-pVTZ and 2.352 Å using MP2/6-311++G(d,p) for the ≡C−H···O bond. The MP2-calculated distance between the C−H hydrogen atom of formic acid to the center of the carbon−carbon triple bond is 2.593 and 2.705 Å with the aug-cc-pVTZ and 6-311++G(d,p) basis sets, respectively. The ≡C−H···O hydrogen-bond distances (2.3−2.4 Å) and nonlinear hydrogen-bond angles are typical for C−H···O-type hydrogen bonds.[42] A similar type of bridged complex with the two subunits bound through two nonlinear hydrogen bonds is the formaldehyde−acetylene complex, which was investigated by rotational spectroscopy.[43] In the formaldehyde−acetylene complex, the cyclic structure arises from a C−H···O and a secondary C−H···π interaction. The hydrogen-bond distances are 2.39 Å (O···H−C) and 3.12 Å (C≡C center···H−C). Using the MP2/6-311++G(d,p) method, we predict another minimum B1 with a single interaction in addition to the structure B. At the B3LYP level of theory (with both the 6-311++G(d,p) and the aug-cc-pVTZ basis set), structure B is not a minimum and the optimization leads to the monodentate structure B1. This suggests that the B3LYP method is not reliable to represent structures with very weak molecular interactions.

TABLE 3: Comparison of Selected Geometric Parameters of Formic Acid, Acetylene, and the Formic Acid−Acetylene Complexes A and B[a]

	parameter	MP2/ aug-cc-pVTZ	MP2/ 6-311++G(d,p)
HCOOH	r(O−H)	0.971	0.969
	r(C−O)	1.347	1.348
	r(C═O)	1.205	1.205
	∠(COH)	106.45	106.34
	∠(O═CO)	125.11	125.20
	∠(O═CH)	125.23	125.28
C_2H_2	r(C≡C)	1.212	1.216
	r(C−H)	1.062	1.065
O−H···π (A)	r(O−H)	0.978	0.974
	r(C−O)	1.339	1.342
	r(C═O)	1.209	1.209
	∠(COH)	107.72	107.26
	∠(O═CO)	125.66	125.62
	r(C≡C)	1.214	1.218
	r(C_1H)	1.063	1.066
	r(C_2H)	1.065	1.067
	r(O−H···center)	2.216	2.304
	r(C−H···O)	2.608	2.733
	∠(C−H···O)	114.60	111.51
C−H···O═C(B)	r(C═O)	1.208	1.208
	r(C−O)	1.342	1.344
	∠(OCO)	124.90	125.03
	r(C≡C)	1.214	1.217
	r(C_2H)	1.066	1.069
	r(C═O···H)	2.278	2.352
	∠(C−H···O)	143.67	143.04

[a] The bond distances are given in Å and bond angles in deg.

As seen from Table 1, the binding energy obtained using MP2/aug-cc-pVTZ is −3.3 kcal/mol, which is reduced to −2.9 after the BSSE correction. After addition of the ZPE correction of 0.8 kcal/mol, the binding energy drops to −2.1 kcal/mol. With the 6-311++G(d,p) basis set, the uncorrected binding energy is −2.9 kcal/mol, which is reduced by −1.5 kcal/mol after correcting for both BSSE and ZPE. There are literature examples of positive binding energies for well-defined minima after both the BSSE and ZPE correction, indicating a possible overcorrection of the actual binding energy.[44,45] As in complex A, the binding energy of complex B is sensitive to the basis set. Compared to complex A, the interaction in complex B is weaker, despite two noncovalent interactions. The comparison of the BSSE-corrected binding energy of complex A with that of complex B at the MP2/aug-cc-pVTZ level shows that A is more stable by 2.0 kcal/mol. The binding energies of complex B1 at the MP2 and B3LYP levels are shown in Tables 1 and 2, respectively. The binding energies obtained by MP2/6-311++G(d,p) and B3LYP/6-311++G(d,p) show only small differences ($\Delta E_{(ZPE)}$ = 1.9 and 1.7 kcal/mol respectively).

In the third complex C, the main interaction is between one hydrogen atom of acetylene and the hydroxyl oxygen atom of formic acid. In addition, there is a weak secondary interaction between the formyl hydrogen atom of formic acid and the π-system of acetylene. The hydrogen-bond distance for the C−H···O−H interaction is 2.501 and 2.578 Å at the MP2/aug-cc-pVTZ and MP2/6-311++G(d,p) level of theory, respectively. The distance between the C−H hydrogen atom of formic acid and the center of the carbon−carbon triple bond is 2.713 Å using MP2/aug-cc-pVTZ and 2.795 Å using MP2/6-311++G(d,p). With MP2/6-311++G(d,p), one more minimum with a single noncovalent interaction is predicted (structure C1). Again, at the DFT level, only the acyclic structure C1 is a minimum.

This resembles the case of the NH_3-H_2O complex for which the DFT method failed to predict the cyclic structure.[46]

The uncorrected binding energy for complex C (MP2/aug-cc-pVTZ) is −2.3 kcal/mol, which is 1.0 kcal/mol less than that of complex B. The BSSE-corrected binding energy is −2.0 kcal/mol, and the ZPE-corrected binding energy −1.8 kcal/mol. The binding energy of structure C1 is not much different from that of C at the MP2/6-311++G(d,p) level (Table 1) but is very low at the DFT level. Selected structural parameters of formic acid and acetylene as monomers and of the two lower-energy complexes are given in Table 3.

Comparison of the Calculated and the Experimental Vibrational Frequencies. The MP2-calculated vibrational frequencies of the monomers and two of the lower-energy cyclic complexes A and B are given in Tables 4 and 7. The calculated vibrational frequencies of acetylene and formic acid that have marked frequency shifts due to the complex formation are compared with the experimentally observed values. Frequencies were computed for the deuterated acetylene complex of formic acid at the MP2/6-311++G(d,p) level, and the computed relative frequency shifts and the experimentally observed relative frequency shifts are compared with that of the formic acid−acetylene complex.

Complex A. As seen from Table 4, the most-perturbed vibrational mode in complex A is the O−H stretching vibration of formic acid. The frequency shift due to complexation is calculated to −139 cm^{-1} at the MP2/aug-cc-pVTZ level and to −98 cm^{-1} at the MP2/6-311++G(d,p) level of theory. The other two vibrational modes of formic acid with marked shifts in complex A are the C═O (−14 cm^{-1}) and the C−O stretching vibration (+38 cm^{-1}, MP2/aug-cc-pVTZ; −11 and +30 cm^{-1}, respectively, with MP2/6-311++G(d,p)). The two vibrational modes of acetylene, the C−H stretching mode and the CCH bending modes, were also perturbed in the complex. The doubly degenerate bending mode of acetylene splits in the complex because of the lifting of degeneracy. The frequency shift for the C−H stretching mode is −19 cm^{-1} and those of the CCH bending modes are +14, and +30 cm^{-1} (MP2/aug-cc-pVTZ). With use of the 6-311++G(d,p) basis set, the frequency shift for the C−H stretching mode is −13 cm^{-1} and those of the CCH bending modes are +12, and +18 cm^{-1}. One of the bending mode frequencies (783.6 cm^{-1}, MP2/aug-cc-pVTZ) exhibits a large frequency shift from the degenerate monomer mode at 753.8 cm^{-1}. This large shift is associated with the coupling between the bending modes of formic acid and acetylene in the complex, as observed for the acetylene dimer.[47]

The calculated frequency shifts of the vibrational modes of formic acid interacting with C_2D_2 and C_2H_2 are basically identical. The relative frequency shifts of the C−D stretching and CCD bending modes of the acetylene unit agree well with the C−H stretching and CCH bending modes as seen from Table 5. The C−D stretching frequency at 2538.6 cm^{-1} is shifted to 2527.4 ($\Delta\nu/\nu = 0.004$), and the bending mode at 561.5 cm^{-1} is shifted to 572.3 and 572.8 cm^{-1} ($\Delta\nu/\nu = 0.019$).

TABLE 5: Comparison of Experimental (Ar matrix at 15 K) and Calculated (MP2/6-311++G(d,p)) Frequency Shifts ($\Delta\nu/\nu$) of the Complexes A and B

complex	experimental		computed		mode of assignment
	C_2H_2	C_2D_2	C_2H_2	C_2D_2	
O−H···π bidentate (A)	0.005	0.005	0.004	0.004	C−H/D stretch
	0.015	0.017	0.015	0.019	CCH/D bend
	0.021	0.019	0.023	0.019	
C−H···OC bidentate (B)	0.012	0.013	0.009	0.007	C−H/D stretch
	0.035	0.030	0.033	0.031	CCH/D bend
	0.044		0.040	0.041	

On codeposition of formic acid and acetylene in solid argon, a few new absorptions are observed that cannot be assigned to the parent species. These new bands appear near the vibrational modes of formic acid and acetylene. The perturbed modes of formic acid indicating the complex formation are found at 3413.3, 1756.6, and 1134.4 cm^{-1} as strong bands (Figures 1−3). The corresponding parent modes are at 3550.4 (O−H str), 1767.1 (C═O str), and 1103.5 cm^{-1} (C−O str). The frequency shifts in the complex are thus −137, −11, and +31 for the O−H, C═O, and C−O stretching vibrations, respectively. The large red shift for the O−H stretching vibration indicates a strong interaction between formic acid and acetylene. It is also evident that the carboxylic group of formic acid is the proton donor in this complex, as predicted by the calculations. The C−H stretching mode of acetylene at 3288.8 cm^{-1} exhibits a red shift of about 15 cm^{-1} in the complex. The CCH bending mode of acetylene at 736.8 cm^{-1} is split, because of the lifting of degeneracy, into two blue-shifted components at 748.1 and 752.7 cm^{-1} in the complex. The frequency shifts for the acetylene vibrational modes are small, which is in accordance with the expectation for a hydrogen-bonded complex when acetylene is the proton acceptor.[38] The experimentally observed frequency shifts are in excellent agreement with that calculated for complex A. One exception is the split CCH bending mode of acetylene obtained by the MP2/aug-cc-pVTZ calculation (Table 4).

The experiments using C_2D_2 confirmed the assignment of the formic acid−acetylene complex A. The C−D stretching mode at 2442.0 cm^{-1} is red-shifted to 2429.1 cm^{-1}, and the bending mode at 542.5 cm^{-1} is blue-shifted to 551.7 and 553.1 cm^{-1}. The relative frequency shifts in the C−D stretching ($\Delta\nu/\nu = 0.005$) and CCD bending modes ($\Delta\nu/\nu = 0.017$ and 0.019) agree well with those obtained in the C_2H_2 experiment ($\Delta\nu/\nu = 0.005$, 0.015, and 0.021, respectively, Table 5).

A comparison of the frequency shifts of the O−H stretching mode of formic acid and the CCH bending mode of acetylene with the π-complexes of acetylene−HX (HF, HCl, and HBr)

TABLE 4: Experimental (Ar matrix at 15 K) and Calculated (MP2) Unscaled Vibrational Frequencies (in cm^{-1}) of the Formic Acid−Acetylene Complex A, along with the Frequency Shifts, $\Delta\nu$, Relative to the Isolated Monomers (in Parentheses)

experimental frequencies		calculated frequencies: MP2/aug-cc-pVTZ		calculated frequencies: MP2/6-311++G(d,p)		
monomer	complex A	monomer	complex A	monomer	complex A	mode of assignment
3550.4	3413.3 (−137)	3740.8	3601.8 (−139)	3797.2	3699.1 (−98)	O−H stretch (ν_1)[a]
1767.1	1756.6 (−11)	1793.7	1779.4 (−14)	1807.5	1796.2 (−11)	C═O stretch (ν_3)[a]
1103.5	1134.4 (+31)	1130.9	1168.5 (+38)	1142.6	1172.9 (+30)	C−O stretch (ν_6)[a]
3288.8	3273.8 (−15)	3431.7	3412.7 (−19)	3455.2	3442.1 (−13)	C−H stretch (ν_3)[b]
736.8	748.1 (+11)	753.8	767.8 (+14)	766.3	778.5 (+12)	CCH bend (ν_5)[b]
	752.7 (+16)		783.6 (+30)		783.8 (+18)	

[a] Formic acid modes in the complex. [b] Acetylene modes in the complex.

systems[36] reveals that the hydrogen-bond strength in the formic acid−acetylene complex is comparable to that of the HBr complex. The red shifts in the HX stretching modes in the π complexes of acetylene were reported to be 215, 124, and 102 cm^{-1}, and the blue shifts for the CCH bending modes were reported to be 21, 15, and 13 cm^{-1} for the π complexes of HF, HCl, and HBr, respectively. The relative frequency shift of the O−H stretching mode of formic acid in the complex ($\Delta\nu/\nu$) is 0.039, close to those observed for the complexes with HBr (0.040) and HCl (0.043). Only in the HF complex the shift is larger (0.054). Figure 10 shows that the experimental infrared spectrum of the formic acid−acetylene complex reasonably agrees with the calculated spectrum of complex A. Only the O−H stretching vibration in the complex A shows a larger deviation.

The vibrational frequencies obtained with B3LYP/aug-cc-pVTZ and B3LYP/6-311++G(d,p) are also compared with the experimental frequencies (Table 6). As in the case of the MP2 calculations, Dunning's basis set leads to an excellent agreement between the calculated and experimentally obtained frequency shifts induced by the complexation.

Complex B. The computed vibrational frequencies of the second minimum B obtained with both basis sets at the MP2 level along with the experimental frequencies are listed in Table 7. In complex B, the perturbation of the formic acid vibrational modes are small compared to complex A. The frequency shifts for the C═O stretching mode are −10 and −9 cm^{-1}, and those for the C−O stretch are +11 and +10 cm^{-1} using MP2/aug-cc-pVTZ and MP2/6-311++G(d,p), respectively. On the basis

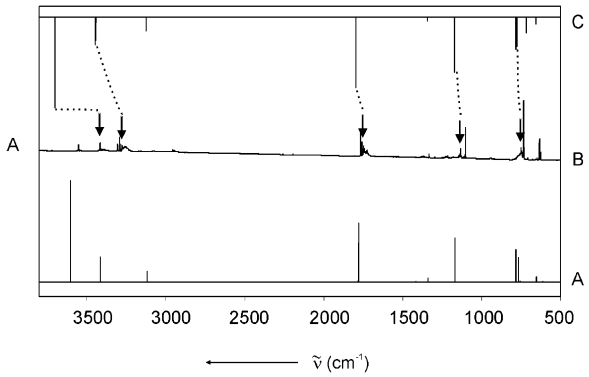

Figure 10. Comparison of matrix isolation infrared spectra of formic acid−acetylene−Ar mixture with the computed spectra of O−H···π complex: (A) MP2/aug-cc-pVTZ; (B) HCOOH−C_2H_2−Ar (1:2:600); (C) MP2/6-311++G(d,p).

TABLE 6: Experimental (Ar matrix at 15 K) and Calculated (DFT/B3LYP) Unscaled Vibrational Frequencies (in cm^{-1}) of the Formic Acid−Acetylene Complex A, along with the Frequency Shifts, $\Delta\nu$, in the Complex Relative to the Isolated Monomers (in Parentheses)

		calculated frequencies				
experimental frequencies		B3LYP/aug-cc-pVTZ		B3LYP/6-311++G(d,p)		
monomer	complex A	monomer	complex A	monomer	complex A	mode of assignment
3550.4	3413.3(−137)	3717.5	3577.3 (−140)	3737.9	3608.6 (−129)	O−H stretch (ν_1)[a]
1767.1	1756.6 (−11)	1811.4	1793.4 (−18)	1816.0	1798.3 (−17)	C═O stretch (ν_3)[a]
1103.5	1134.4 (+31)	1121.4	1155.3 (+34)	1125.5	1157.4(+32)	C−O stretch (ν_6)[a]
3288.8	3273.8 (−15)	3412.2	3395.8 (−16)	3419.7	3402.0 (−18)	C−H stretch (ν_3)[b]
736.8	748.1 (+11)	769.4	784.7 (+15)	772.8	788.7 (+16)	CCH bend (ν_5)[b]
	752.7 (+16)		794.9 (+26)		798.0 (+25)	

[a] Formic acid modes in the complex. [b] Acetylene modes in the complex.

TABLE 7: Experimental (Ar matrix at 15 K) and Calculated (MP2) Unscaled Vibrational Frequencies (in cm^{-1}) of the Formic Acid−Acetylene Complex B, along with the Frequency Shifts $\Delta\nu$ in the Complex Relative to the Isolated Monomers (in Parentheses)

		calculated frequencies				
experimental frequencies		MP2/aug-cc-pVTZ		MP2/6-311++G(d,p)		
monomer	complex B	monomer	complex B	monomer	complex B	mode of assignment
3550.4		3740.8	3738.4 (−2)	3797.7	3795.3 (−2)	O−H stretch (ν_1)[a]
1767.1	1761.6 (−6)	1793.7	1783.3 (−10)	1807.6	1798.5 (−9)	C═O stretch (ν_3)[a]
1103.5	1114.5 (+11)	1130.9	1141.8 (+11)	1142.7	1152.8 (+10)	C−O stretch (ν_6)[a]
3288.8	3248.6 (−40)	3431.7	3390.7 (−41)	3457.6	3428.1 (−30)	C−H stretch (ν_3)[b]
736.8	764.0 (+27)	753.8	792.7 (+39)	764.8	790.5 (+26)	CCH bend (ν_5)[b]
	770.7 (+34)		793.5 (+40)		797.2 (+32)	

[a] Formic acid modes in the complex. [b] Acetylene modes in the complex.

TABLE 8: Experimental (Ar matrix at 15 K) and Calculated (DFT/B3LYP) Unscaled Vibrational Frequencies (in cm^{-1}) of the Formic Acid−Acetylene Complex B1, along with the Frequency Shifts, $\Delta\nu$, in the Complex Relative to the Isolated Monomers (in Parentheses)

		calculated frequencies				
experimental frequencies		B3LYP/aug-cc-pVTZ		B3LYP/6-311++G(d,p)		
monomer	complex B1	monomer	complex B1	monomer	complex B1	mode of assignment
3550.4		3717.5	3713.7 (−4)	3737.9	3734.7 (−3)	O−H stretch (ν_1)[a]
1767.1	1761.6 (−6)	1811.4	1801.5 (−10)	1816.0	1805.3 (−10)	C═O stretch (ν_3)[a]
1103.5	1114.5 (+11)	1121.4	1133.2 (+12)	1125.5	1138.8 (+13)	C−O stretch (ν_6)[a]
3288.8	3248.6 (−40)	3412.2	3374.8 (−37)	3419.7	3379.5 (−40)	C−H stretch (ν_3)[b]
736.8	764.0 (+27)	769.4	823.5 (+54)	772.8	832.8 (+60)	CCH bend (ν_5)[b]
	770.7 (+34)		824.1 (+55)		836.6 (+64)	

[a] Formic acid modes in the complex. [b] Acetylene modes in the complex.

of these calculations the weak bands at 1761.6 and 1114.5 cm^{-1} were assigned to the perturbed modes of the C═O and C−O stretching vibrations of formic acid in complex B. The low intensity of these modes indicates that the concentration of this complex is much less than that of complex A. Other modes of the formic acid unit could not be detected. With deuterated acetylene, the C═O stretching mode of complex B gained in intensity (Figure 2C).

In complex B, the C−H stretching mode of acetylene is predicted to shift by −41 cm^{-1} (MP2/aug-cc-pVTZ, −30 cm^{-1} with MP2/6-311++G(d,p), Table 7). The frequency shifts for the CCH bending mode are calculated to be +39 and +40 cm^{-1} with MP2/aug-cc-pVTZ and +26 and +32 cm^{-1} with MP2/6-311++G(d,p). Again, the deuteration of acetylene results in similar calculated relative shifts induced by the complex formation (Table 5).

The perturbed acetylene modes are also very weak in the matrix experiment. The C−H stretching mode appears at 3248.6 cm^{-1}, red-shifted by 40 cm^{-1}, in excellent agreement with the shift calculated at the MP2/aug-cc-pVTZ level of theory. The bending modes appeared at 764.0 and 770.7 cm^{-1}, blue-shifted by 27 and 34 cm^{-1}. The large complex-induced shifts in the acetylene subunit are a clear evidence for the presence of a C−H···O═C complex, where acetylene is the proton donor. These results are confirmed in the experiments using C_2D_2 where the C−D stretching mode is shifted from 2442.0 to 2411.5 cm^{-1} and the CCD bending mode from 542.5 to 559.9 cm^{-1}.

A comparison of the frequency shifts for similar hydrogen-bonded systems such as water−acetylene or acetone−acetylene indicates that the ≡C−H···O interaction in the formic acid−acetylene complex B is weaker than that in the water−acetylene or the acetone−acetylene complex. In water−acetylene, the perturbed CH stretching mode appears at 3240.2 cm^{-1} (a red shift of 49 cm^{-1}),[39] and in the acetone complex the red-shift is 69 cm^{-1}.[14] The frequency shifts for the ≡CH stretching mode induced by the interaction with water and formic acid are comparable, but in acetone, the shift is larger. The corresponding bending modes in the acetylene−water complex appear at 793 and 786 cm^{-1} and in the acetone complex at 790 and 774 cm^{-1}. Generally, the magnitude of frequency shifts is correlated with the hydrogen-bond strength, and such comparison indicates that the C−H···O interaction in the formic acid−acetylene complex B is weaker than in the water−acetylene and acetone−acetylene complexes.

Table 8 lists the calculated vibrational frequencies of the second minimum, complex B1, obtained with B3LYP, along with the experimental frequencies. Except for the CCH bending mode of the acetylene subunit, the calculated vibrational modes are in fairly good agreement with the experimental frequencies. The very large deviation of the CCH bending mode (about a factor of 2) clearly indicates that the experimental spectrum is not in accordance with the structure B1. For the CCH bending mode, the calculated frequency shift for the B1 structure obtained by the MP2/6-311++G(d,p) method is about three times larger than the experimental shift. The mismatch between the experimental and calculated shifts for the B1 structure is a clear indication that the cyclic structure B obtained by the MP2 method is the actual C−H···O═C complex B observed in the argon matrix.

Comparison of the Structural Parameters and the Frequency Shifts. The extent of bond lengthening or shortening correlates very well with the amount of red or blue shifts observed in the corresponding vibrational modes on complex formation. The changes in the structural parameters of the monomers due to complex formation are relatively small (Table 3). In the O−H···π complex A, the largest changes occur for the O−H and C−O bond, r(O−H) lengthened by 0.007 Å and r(C−O) shortened by 0.008 Å, and this agrees with the maximum frequency shifts for the O−H (toward red) and C−O (toward blue) stretching vibrations. The $r(C_1H)$ is lengthened by 0.001 Å, whereas $r(C_2H)$ is lengthened by 0.003 Å in complex A, an additional evidence for the secondary interaction involving one hydrogen atom of acetylene and the carbonyl oxygen of formic acid. In the C−H···O═C complex B, the bond length of the donor C−H group, $r(C_2H)$, lengthened by 0.004 Å, in agreement with the maximum frequency shift for the C−H stretch of acetylene compared to the observed shift in O−H···π complex.

Conclusions

The matrix isolation technique, combined with ab initio computations, has been used to characterize the 1:1 complexes of formic acid and acetylene. Three stable complexes with cyclic geometries were identified at the MP2 level of theory. The global minimum structure A has O−H···π and C−H···O═C interactions in the same complex. The most convincing evidence for the O−H···π interaction is the large red shift of the O−H stretching vibration of the formic acid subunit. The experimentally observed frequency shift for the O−H stretching vibration is in excellent agreement with the frequency shift calculated using MP2/aug-cc-pVTZ theory. A large binding energy is always paralleled by large frequency shifts due to the complex formation. While the strong O−H···π interaction is well described by both MP2 and DFT, the C−H···π interaction was only reproduced correctly at the MP2 level of theory. The BSSE-corrected binding energy of the global minimum structure A is −4.9 kcal/mol and that of the C−H···O═C complex B is −2.9 kcal/mol (MP2/aug-cc-pVTZ). These two low-energy complexes were identified in the matrix experiments using both C_2H_2 and C_2D_2 to confirm the assignment of the IR spectra. The experimentally observed vibrational frequency shifts of the modes of formic acid and acetylene induced by the complexation are in good agreement with the calculated values.

Acknowledgment. The financial support from the Deutsche Forschungsgemeinschaft (SFB 452) and the Fonds der Chemischen Industrie is gratefully acknowledged. We thank Dr. Holger Bettinger for fruitful discussions and manuscript suggestions.

References and Notes

(1) Steiner, T. *J. Phys. Chem. A* **2000**, *104*, 433.
(2) Desiraju, G. R. *Acc. Chem. Res.* **1996**, *29*, 441.
(3) Sankaran, K.; Vidya, V.; Viswanathan, K. S.; George, L.; Singh, S. *J. Phys. Chem. A* **1998**, *102*, 2944.
(4) Rablen, P. R.; Lockman, J. W.; Jorgensen, W. L. *J. Phys. Chem. A* **1998**, *102*, 3782.
(5) Van Bael, M. K.; Smets, J.; Schoone, K.; Houben, L.; McCarthy, W.; Adamowicz, L.; Nowak, M. J.; Maes, G. *J. Phys. Chem. A* **1997**, *101*, 2397.
(6) Mmereki, B. T.; Donaldson, D. J. *J. Phys. Chem. A* **2002**, *106*, 3185.
(7) Desiraju, G. R.; Steiner, T. *The Weak Hydrogen Bond in Structural Chemistry and Biology*; Oxford University Press: Oxford, U.K., 1999.
(8) Grabowski, S. *J. Phys. Chem. A* **2002**, *105*, 10746.
(9) Jeffrey, G. A.; Malluszynska, H. *Int. J. Biol. Macromol.* **1982**, *4*, 173.
(10) Sundararajan, K.; Vidya, V.; Sankaran, K.; Viswanathan, K. S. *Spectrochim. Acta A* **2000**, *56*, 1855.
(11) Hartmann, M.; Wetmore, S. D.; Radom, L. *J. Phys. Chem. A* **2001**, *105*, 4470.
(12) Tsuzuki, S.; Honda, K.; Uchimaru, T.; Mikami, M.; Tanabe, K. *J. Am. Chem. Soc.* **2000**, *122*, 3746.

(13) Jeng, M. H.; Delaat, A. M.; Ault, B. S. *J. Phys. Chem*. **1989**, *93*, 3997.
(14) Delaat, A. M.; Ault, B. S. *J. Am. Chem. Soc*. **1987**, *109*, 4232.
(15) Jeng, M. H.; Ault, B. S. *J. Phys. Chem.* **1990**, *94*, 4851.
(16) Tsuzuki, S.; Honda, K.; Uchimaru, T.; Mikami, M.; Tanabe, K. *J. Am. Chem. Soc*. **2000**, *122*, 11450.
(17) Samanta, U.; Chakrabarti, P.; Chandrasekhar, J. *J. Phys. Chem. A* **1998**, *102*, 8964.
(18) Frisch, M. J.; Trucks, G. W.; Schlegel, H. B.; Scuseria, G. E.; Robb, M. A.; Cheeseman, J. R.; Zakrzewski, V. G.; Montgomery, J. A., Jr.; Stratmann, R. E.; Burant, J. C.; Dapprich, S.; Millam, J. M.; Daniels, A. D.; Kudin, K. N.; Strain, M. C.; Farkas, O.; Tomasi, J.; Barone, V.; Cossi, M.; Cammi, R.; Mennucci, B.; Pomelli, C.; Adamo, C.; Clifford, S.; Ochterski, J.; Petersson, G. A.; Ayala, P. Y.; Cui, Q.; Morokuma, K.; Malick, D. K.; Rabuck, A. D.; Raghavachari, K.; Foresman, J. B.; Cioslowski, J.; Ortiz, J. V.; Stefanov, B. B.; Liu, G.; Liashenko, A.; Piskorz, P.; Komaromi, I.; Gomperts, R.; Martin, R. L.; Fox, D. J.; Keith, T.; Al-Laham, M. A.; Peng, C. Y.; Nanayakkara, A.; Gonzalez, C.; Challacombe, M.; Gill, P. M. W.; Johnson, B. G.; Chen, W.; Wong, M. W.; Andres, J. L.; Head-Gordon, M.; Replogle, E. S.; Pople, J. A. *Gaussian 98*, revision A.11; Gaussian, Inc.: Pittsburgh, PA, 1998.
(19) Møller, C.; Plesset, M. S. *Phys. Rev.* **1934**, *46*, 618.
(20) Becke, A. D. *J. Chem. Phys.* **1993**, *98*, 5648.
(21) Lee, C.; Yang, W.; Parr, R. G. *Phys. Rev. B* **1988,** *37*, 785.
(22) Krishnan, R.; Brinkley, J. S.; Seeger, R.; Pople, J. A. *J. Chem. Phys*. **1980**, *72*, 650.
(23) Frisch, M. J.; Pople, J. A.; Brinkley, J. S. *J. Chem. Phys*. **1984**, *80*, 3265.
(24) Dunning, T. H., Jr. *J. Chem. Phys.* **1989**, *90*, 1007.
(25) Boys, S. F.; Bernardi, F. *Mol. Phys.* **1970**, *19*, 553.
(26) Montero, L. A.; Esteva, A. M.; Molina, J.; Zapardiel, A..; Hernández, L.; Márquez, H.; Acosta, A. *J. Am. Chem. Soc*. **1998**, *120*, 12023.
(27) Montero, L. A.; Molina, J.; Fabian, J. *Int. J. Quantum Chem.* **2000**, *79*, 8.
(28) Montero, L. A. GRANADA and Q Programs for PC computers, 1996 (available on request).
(29) Reva, I. D.; Plokhotnichenko, A. M.; Radchenko, E. D.; Sheina, G. G.; Blagoi, Yu. P. *Spectrochim. Acta A* **1994**, *50*, 1107.
(30) Lundell, J.; Räsänen, M.; Latajka, Z. *Chem. Phys*. **1994**, *189*, 245.
(31) Redington, R. L. *J. Mol. Spectrosc*. **1977**, *65*, 171.
(32) Pettersson, M.; Lundell, J. *J. Am. Chem. Soc*. **1997**, *119*, 11715.
(33) Halupka, M.; Sander, W. *Spectrochim. Acta, Part A* **1998**, *54*, 495.
(34) Gantenberg, M.; Halupka, M.; Sander, M. *Chem.—Eur. J*. **2000**, *6*, 1865.
(35) Kline, E. S.; Kafafi, Z. H.; Hauge, R. H.; Margrave, J. L. *J. Am. Chem. Soc*. **1985**, *107*, 7559.
(36) McDonald, S. A.; Johnson, G. L.; Keelan, B. W.; Andrews, L. *J. Am. Chem. Soc.* **1980**, *102*, 2892.
(37) Lundell, J.; Räsänen, M. *J. Phys. Chem*. **1995**, *99*, 14301.
(38) Jemmis, E. D.; Giju, K. T.; Sundararajan, K.; Sankaran, K.; Vidya, V.; Viswanathan, K. S.; Leszczynski, J. *J. Mol. Struct*. **1999**, *510*, 59.
(39) Engdahl, A.; Nelander, B. *Chem. Phys. Lett*. **1983**, *100*, 129.
(40) Grabowski, S. J. *J. Phys. Chem. A* **2001**, *105*, 10739.
(41) Feyereisen, M. W.; Feller, D.; Dixon, D. A. *J. Phys. Chem*. **1996**, *100*, 2993.
(42) Cabaleiro-Lago, E. M.; Otero, J. R**.** *J. Chem. Phys***.** ***2002***, *117*, 1621.
(43) Howard, N. W.; Legon, A. C. *J. Chem. Phys.* **1988**, *88*, 6793.
(44) Turi, L.; Dannenberg, J. J. *J. Phys. Chem.* **1993**, *97*, 7899.
(45) Sundararajan, K.; Sankaran, K.; Viswanathan, K. S.; Kulkarni, A. D.; Gadre, S. R. *J. Phys. Chem. A* **2002**, *106*, 1504.
(46) Sadlej, J.; Moszynski, R.; Dobrowolski, J. Cz.; Mazurek, A. P. *J. Phys. Chem. A* **1999**, *103*, 8528.
(47) Pendley, R. D.; Ewing, G. E. *J. Chem. Phys.* **1983**, *78*, 31.